

Electromyography Pattern Classification with Laplacian Eigenmaps in Human Running

Elnaz Lashgari, Emel Demircan

Abstract—Electromyography (EMG) is one of the most important interfaces between humans and robots for rehabilitation. Decoding this signal helps to recognize muscle activation and converts it into smooth motion for the robots. Detecting each muscle's pattern during walking and running is vital for improving the quality of a patient's life. In this study, EMG data from 10 muscles in 10 subjects at 4 different speeds were analyzed. EMG signals are nonlinear with high dimensionality. To deal with this challenge, we extracted some features in time-frequency domain and used manifold learning and Laplacian Eigenmaps algorithm to find the intrinsic features that represent data in low-dimensional space. We then used the Bayesian classifier to identify various patterns of EMG signals for different muscles across a range of running speeds. The best result for vastus medialis muscle corresponds to 97.87 ± 0.69 for sensitivity and 88.37 ± 0.79 for specificity with 97.07 ± 0.29 accuracy using Bayesian classifier. The results of this study provide important insight into human movement and its application for robotics research.

Keywords—Electrocardiogram, manifold learning, Laplacian Eigenmaps, running pattern.

I. INTRODUCTION

IMPROVING the accuracy of synthesized human motion is an ongoing challenge in various disciplines such as neuroscience [1], physiology, biomechanics [2], brain computer interface [3], and robotics [4], [5]. In such applications, feasible sensing technologies such as EMG, cortical neural implants, and human motion reconstruction provide some channels for interface. These fields attempt to decode these neural activities and map them into movement commands for devices such as robots [6], [7]. Therefore, finding an effective way for decoding the neuromuscular activities with the purpose of accurate modeling and recognition of motion patterns will help convert kinematic variables to smooth motion for a robot [8], [9].

Investigating EMG patterns during walking and running at different speeds is a popular research question of many studies [10]-[12]. The EMG patterns of leg muscles during stride have been used to clinically assess injury [13], and prevent disease by designing sport shoes [14]. These patterns have different morphologies during walking and running at different speeds

[15].

By finding similarities between EMG patterns at different speeds, the number of basic functions for running can be reduced. On the other hand, EMG signals are complex and nonlinear, and the challenge faced by analyzing these signals is the range of variation of its patterns. Multivariate EMG data are noisy and redundant. Therefore, extracting significant features and representing the underlying structure in an efficient way is important [16], [17]. Several methods were used to classify the profile of EMG during running. In this study, instead of working with points with high-dimensionality features, we applied Manifold learning and the Laplacian Eigenmaps algorithm to find intrinsic features [18]. The relationships between EMG and ground reaction forces were investigated at four speeds, for 10 important muscles (in running) with 10 male subjects. We discovered that the Laplacian Eigenmaps nonlinear dimensionality reduction algorithm is the most appropriate method to reduce the high dimensionality of EMG signals while preserving aspects in time-frequency domain [19].

Our goal was to precisely classify EMG signal, which affects the dynamics of a human body at different running speeds. The results of our simulation can be used in the role of each muscle in supporting or propelling the skeletal system, physical therapy, assessment of injury, and design of sport shoes.

II. METHODS

We used 10 EMG channel data from 10 subjects and ground reaction forces which occurred during running at different speeds on a treadmill [20]. In post processing step we denoised and normalized the EMG signals, then extracted features in time-frequency domain, which formed our input matrix for the manifold learning algorithm.

A. Subjects and Protocol

In this study, we used the data collected at Stanford University [20]. The data set included EMG signals of ten subjects running on a treadmill at four speeds: 2.0, 3.0, 4.0, and 5.0 m/s. Each subject was an experienced long distance runner and all of them were male with average mass, height and age of 71 kg, 1.77m and 30 years, respectively.

B. Post-Processing

EMG signals were recorded with surface electrodes (Delsys Bagnoli system). Ten selected muscles that play an important role in running are: Gluteus maximus (on line between greater trochanter and sacrum), gluteus medius (on line between greater trochanter and crista iliaca), biceps femoris-long head

Elnaz Lashgari is PhD student in California State University, Long Beach with the Mechanical and Aerospace Engineering Department CA 90840-8306 USA (e-mail: elnaz.lashgari@csulb.edu).

Dr. Emel Demircan is assistant professor with the Mechanical and Aerospace Engineering Department, California State University, Long Beach, CA 90840-8306 USA (phone: 562-985-1520; fax: 562-985-4408; e-mail: emel.demircan@csulb.edu).

Research is supported by California State University Long Beach Small Faculty Grant and Alumni Grant.

(dorsomedial side of thigh), vastus lateralis (anterolateral muscle bulge thigh), vastus medialis (anteromedial muscle bulge thigh), tibialis anterior (ventral side of lower leg, just lateral from tibia), gastrocnemius lateralis (middle of muscle bulge), gastrocnemius medialis (middle of muscle bulge), soleus (medial and anterior from achilles tendon), rectus femoris (between vastus medialis and vastus lateralis).

The EMG signal appears random in nature and it is difficult to obtain high-quality electrical signals from EMG sources because the signals typically have low amplitude (in range of mV) and are easily corrupted by noise during recording. Before feature extraction, the EMG signal should be processed to suppress the noise. The most conventional technique for denoising is filtering or smoothing methods [21], [22]. The post-processing of EMG signal included using a 4th order Butterworth high-pass filter with cut-off frequency 20 Hz with a zero-phase, full-wave rectification, and a Butterworth low-pass filter with 4th order and cut-off frequency 24 Hz with a zero-phase, it was corrected for offset and normalized. Fig. 1 represents the stages in post-processing of raw EMG of biceps femoris long head during running with speed of 2 m/s. Fig. 2 shows basic pattern of EMG during running for one subject (Subject 2). In running, muscles can be divided into groups according to their pattern in time domain [10]. Calf group includes; soleus, gastrocnemius medialis, and gastrocnemius lateralis, which have major differences between walking and running. Vastus medialis, vastus lateralis and rectus femoris are in the quadriceps group. While the profiles were identical, the speed dependence was not; their amplitude hardly changed with increasing speed.

Gluteus medius and gluteus maximus are from the gluteal group. At low speed there is one peak in the pattern. By increasing the speed the gluteal group profiles consist of 2 peaks, which linearly increase with speed. Tibialis anterior is a separate group, which completes the swing phase of stride.

In Fig. 3 we represented the pattern of de-noised and normalized gastrocnemius medialis EMG signals at different speeds of 2, 3, 4, and 5 m/s.

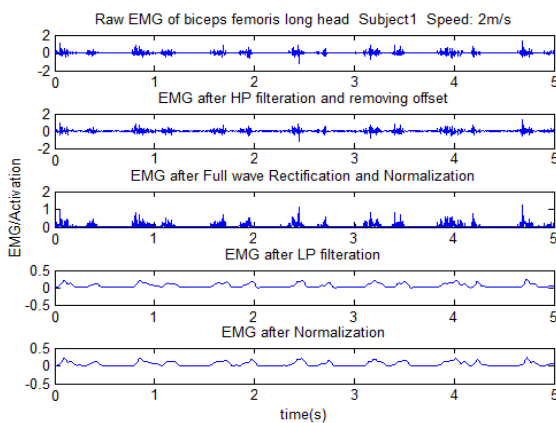


Fig. 1 Post-processing of raw EMG of biceps femoris long head during running at speed 2 m/s

C. Feature Selection

To demonstrate the proposed approach, a total of 50 segments were selected for each muscle of different subjects, where these segments provide our dataset utilized in this study. The EMG segments included intervals of one period on running which is approximately 1 second and included one stride [23]. For this purpose we used an efficient algorithm of Automatic Peak Detection, which is designed for noisy and periodic signals [32]. After defining our segments we needed to interpolate all segments to 500 points to make them the same size, considering all their features.

D. Feature Extraction

In this paper we extracted features in time-frequency domain [24], [25]. The time domain features included the interpolated points in each segment, which corresponds to the amplitude of filtered EMG signals. Then we extracted features in frequency domain as the following:

- Autoregressive coefficients: describe each of EMG segment as a linear combination of previous samples plus a white noise error term.

$$x_n = -\sum_{i=1}^P a_i x_{n-i} + \omega_n$$

- Mean frequency

$$\sum_{j=1}^M f_j P_j \sum_{j=1}^M P_j$$

- Median frequency

$$\sum_{j=1}^{MDF} P_j = \sum_{j=MDF}^M P_j = 1/2 \sum_{j=1}^M P_j$$

Multivariate EMG signals are highly redundant. Representing useful and significant features in low dimensional space shows that the underlying structures is a major task. Manifold learning simplified the issue to find the intrinsic features of EMG sets.

C. Manifold Learning and Laplacian Eigenmaps Algorithm

Complex and non-linear data sets are hard to study in their original form; scientists try to find meaningful low-dimensional data, which is hidden in their high dimensional form. Several algorithms have been proposed to analyze the structure of high-dimensional data based on the notion of manifold learning. These algorithms have been used to extract the intrinsic characteristics of different types of high-dimensional data by performing nonlinear dimensionality reduction such as ISOMAP [18], local linear embedding (LLE) [26] and Laplacian Eigenmaps [19].

All these approaches are completed in 3 main stages:

1. Construct neighborhood graph: Define graph G over all data points i and j which measured by $d_x(i, j)$ and set edge lengths equal to $d_x(i, j)$.
2. Compute shortest paths: Initialize $d_G(i, j) = d_x(i, j)$ if i, j are linked by an edge, $d_x(i, j) = \infty$ otherwise, then for each value of K compute $d_G(i, j)$ and find the final matrix

which contains the shortest path distances between all pairs of data in G .

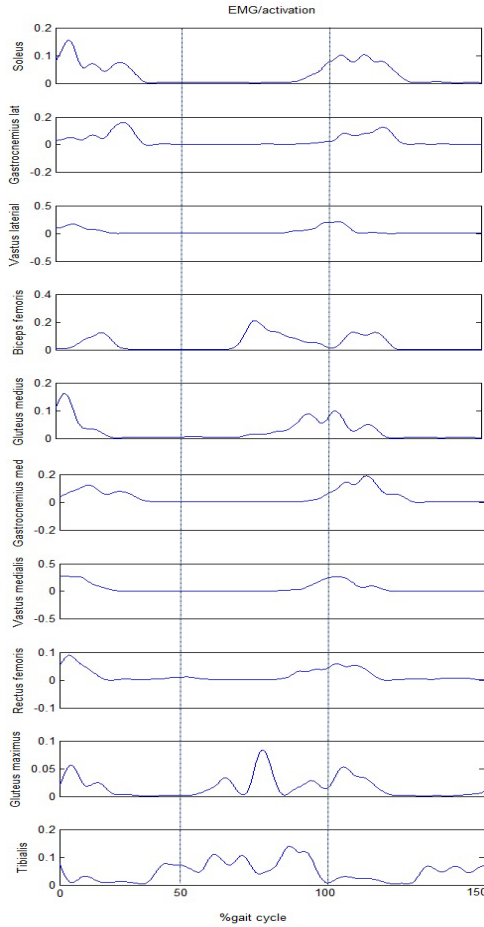


Fig. 2 Patterns of 10 EMG signals in time domain for subject2 during running at speed 2 m/s

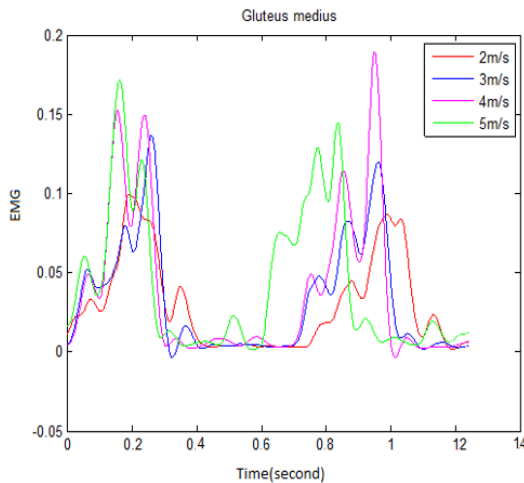


Fig. 3 EMG Pattern of Gluteus medius pattern at four different speeds 2, 3, 4 and 5 m/s

3. Construct d-dimensional embedding: Let λ_p be the p-th eigenvalue in decreasing order of the matrix and v_i^p be the i-th component of the p-th eigenvector. Then set the p-th component of the d-dimensional coordinate vector y_i equal to $\sqrt{\lambda_p} v_i^p$.

We found that the nonlinear dimensionality reduction algorithm “Laplacian Eigenmaps” was the most appropriate method to reduce the high dimensionality of the EMG signals while preserving its properties. The algorithm for Laplacian Eigenmaps is formally stated below [19], [23].

Step1. (Constructing the adjacency graph). We put an edge between nodes i and j if x_i and x_j are “close”. There are two variations:

- i. ϵ -neighborhoods (parameter $\epsilon \in \mathbb{R}$). Nodes i and j are connected to each other by an edge if $\|x_i - x_j\|^2 < \epsilon$ (the Euclidean norm) in \mathcal{R}^D . The advantage of this method is that it is geometrically motivated, the relationship is naturally symmetric. The drawback of this method: it often leads to graphs with several connected components, which make it difficult to choose ϵ .
- ii. K nearest neighbors ($K \in \mathbb{N}$). Nodes i and j are connected by an edge if i is among K nearest neighbors of j and always this relation is symmetric. In this paper we use this method.

Advantages: Simplification of the selection process. This method has a smaller probability of disconnected graphs.

Disadvantages: Geometrically less instinctive

Step2. (Choosing the weights). Here we also have two variations for weighing the edges:

- i. Heat kernel (parameter $t \in \mathbb{R}$). If nodes i and j are connected, put $W_{ij} = e^{-\frac{\|x_i - x_j\|^2}{t}}$ otherwise, put $W_{ij} = 0$.
- ii. Simple-minded (no parameters ($t = \infty$)). $W_{ij} = 1$ if vertices i and j are connected by an edge and $W_{ij} = 0$ if vertices i and j are not connected by an edge. This simplification avoids the need to choose t .

Step3. (Eigenmaps). Assume graph G , depicted above, is a continuous function. Otherwise, proceed with step 3 for every individually connected data. Obtain eigenvalues and eigenvectors for the problem.

$$Lf = \lambda Df$$

where D is symmetric diagonal weight matrix, and its entries are column sums of W , $D_{ii} = \sum_j W_{ji}$. $L = D - W$ is the Laplacian matrix which is symmetric, positive semi definite matrix that can be as an operator on functions defined on vertices of G .

Let f_0, f_1, \dots, f_{n-1} be the solutions of $Lf = \lambda Df$ ordered according to their eigenvalues:

$$\begin{aligned} Lf_0 &= \lambda_0 Df_0 \\ Lf_1 &= \lambda_1 Df_1 \\ &\dots \\ Lf_{n-1} &= \lambda_{n-1} Df_{n-1} \\ 0 &= \lambda_0 \leq \lambda_1 \leq \dots \leq \lambda_{n-1}. \end{aligned}$$

We leave out the eigenvector f_0 corresponding to eigenvalue 0 and use the next d eigenvectors for embedding in d -dimensional Euclidean space: $x_i \rightarrow (f_i(i), \dots, f_d(i))$.

III. RESULTS

A. Pattern of Each Muscle at Different Speeds

In Fig. 3 we represented the EMG pattern of the gluteus medius of one subject (Subject 1) at different speeds. By training Laplacian Eigenmaps algorithm we generalized the result of changing EMG pattern at various speeds. Each subject has 5 stride-EMG records at 4 different speeds. So we used 200 segments for the input matrix of Manifold learning and set $k=20$ which shows nearest neighborhoods. Each segment has 503 features in the time-frequency domain. Fig. 4 shows the output of the algorithm in 2-D Cartesian space for the vastus medialis muscle.

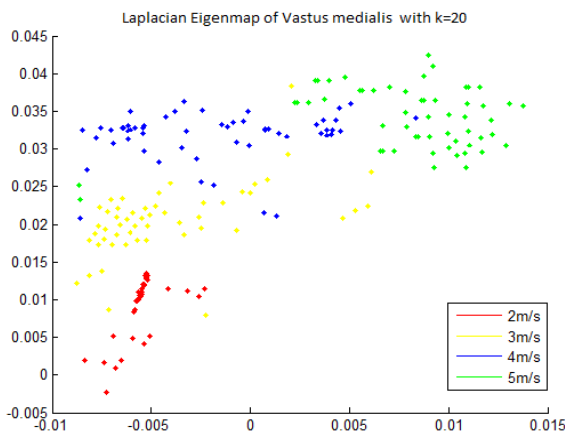


Fig. 4 Laplacian Eigenmaps of vastus medialis with $k=20$ at 4 different speeds

For the classification, nearest neighborhood (NN) [27], Fisher Linear Discriminate Analysis (FLDA) [28] and the Bayesian classifier [29], [30] were employed to evaluate and compare the classification performance by different classifiers. Cross-validation procedure with 5 fold and 10 run was applied to evaluate the classification accuracy. The recognition performance of system was measured by accuracy, sensitivity and specificity [31]. The mean and standard deviations for the specified measures were evaluated and compared. The best result for each muscle is shown in Table I for different k and different classifiers for vastus medialis. The effect of change of EMG activities at different speeds can be reflected in accuracy. The best result for this muscle is indicated in bold and corresponds to 97.87 ± 0.69 for sensitivity and 88.37 ± 0.79 for specificity with 97.07 ± 0.29 accuracy with Bayesian classifier.

Table II shows a similar result for other muscles with $k=20$ and Bayesian classifier.

TABLE I
LAPLACIAN EIGENMAPS FOR EMG OF VASTUS MEDIALIS FOR DIFFERENT K AND BAYESIAN, NN AND FLDA CLASSIFIERS

K	Sensitivity	Specificity	Accuracy	
5	93.12 ± 0.37	86.66 ± 1.24	96.98 ± 0.27	Bayesian
10	95.21 ± 0.32	84.55 ± 0.23	96.41 ± 0.53	
15	96.25 ± 0.26	85.66 ± 1.09	96.94 ± 0.89	
20	97.87 ± 0.63	88.37 ± 0.79	97.07 ± 0.29	
40	97.32 ± 0.21	81.61 ± 1.04	97.31 ± 0.34	
60	97.58 ± 0.25	83.25 ± 1.32	95.73 ± 0.39	
80	96.34 ± 1.12	81.26 ± 1.12	95.23 ± 1.18	
100	96.12 ± 0.98	81.95 ± 1.22	95.95 ± 0.23	
150	96.23 ± 1.54	82.29 ± 1.34	95.67 ± 1.32	
200	95.12 ± 0.07	79.01 ± 1.04	95.87 ± 0.25	
K	Sensitivity	Specificity	Accuracy	
5	92.22 ± 0.32	83.64 ± 0.44	93.97 ± 1.78	Nearest Neighborhood
10	92.37 ± 0.46	83.35 ± 0.53	93.61 ± 1.75	
15	93.45 ± 0.21	85.56 ± 1.06	94.34 ± 0.84	
20	93.76 ± 0.98	85.55 ± 0.69	94.17 ± 0.49	
40	93.98 ± 0.27	86.12 ± 1.66	92.23 ± 0.22	
60	93.45 ± 0.35	86.23 ± 0.72	94.97 ± 0.29	
80	92.54 ± 1.14	85.98 ± 0.92	94.67 ± 0.99	
100	92.34 ± 0.38	85.55 ± 1.22	93.32 ± 0.98	
150	92.45 ± 1.58	85.45 ± 0.56	93.33 ± 0.36	
200	91.65 ± 0.87	84.06 ± 1.94	93.47 ± 0.54	
K	Sensitivity	Specificity	Accuracy	
5	94.45 ± 1.02	86.34 ± 0.39	94.91 ± 0.32	FLDA
10	93.32 ± 1.23	86.65 ± 0.56	94.91 ± 0.72	
15	94.76 ± 0.54	86.97 ± 1.76	94.24 ± 0.34	
20	95.54 ± 0.34	86.43 ± 0.34	95.35 ± 0.76	
40	95.11 ± 0.67	86.23 ± 0.25	95.36 ± 0.28	
60	95.23 ± 0.87	86.56 ± 0.28	95.46 ± 0.23	
80	94.98 ± 1.65	84.98 ± 0.67	94.12 ± 0.19	
100	94.54 ± 0.43	83.55 ± 1.23	93.87 ± 0.98	
150	93.76 ± 1.24	80.45 ± 0.24	93.34 ± 0.87	
200	90.34 ± 1.98	77.26 ± 2.34	93.76 ± 0.94	

This study utilized a PC based system and Matlab R2012b code on a 2.53 GHz Intel® Core™2 Duo CPU, the typical processing time was in the range of 30 seconds for the proposed method.

B. Classification of Groups of Muscles at Each Speed

TABLE II
LAPLACIAN EIGENMAPS FOR EMG OF 10 SELECTED MUSCLES WITH $K=20$ AND BAYESIAN CLASSIFIER

EMG classification of muscles in different speed	Laplacian Eigenmaps for $K=20$ and Bayesian classifier		
	Sensitivity	Specificity	Accuracy
soleus	98.10 ± 0.34	89.10 ± 0.33	97.01 ± 0.52
gastrocnemius medialis	98.98 ± 0.62	90.61 ± 0.44	96.61 ± 0.42
gastrocnemius lateralis	98.02 ± 0.56	88.55 ± 0.16	96.18 ± 0.82
vastus medialis	97.87 ± 0.69	88.37 ± 0.79	97.07 ± 0.29
vastus lateralis	97.32 ± 0.21	86.92 ± 0.91	98.54 ± 1.01
rectus femoris	98.03 ± 0.61	89.15 ± 0.56	98.32 ± 0.54
biceps femoris-long head	99.05 ± 0.01	91.65 ± 0.23	98.65 ± 0.02
gluteus medius	98.45 ± 0.84	92.74 ± 0.84	97.70 ± 0.84
gluteus maximus	98.71 ± 0.24	92.70 ± 0.24	96.70 ± 0.12
tibialis anterior	98.70 ± 0.64	93.31 ± 0.78	93.32 ± 0.14

In this study, we investigated different patterns of EMG signals of different subjects at specific speeds. This issue is important to classify the contribution of each muscle to body

mass-center accelerations.

The input matrix for training our algorithm consists of 500 rows and consisting of 503 features. Fig. 5 shows the results of the Laplacian Eigenmaps algorithm.

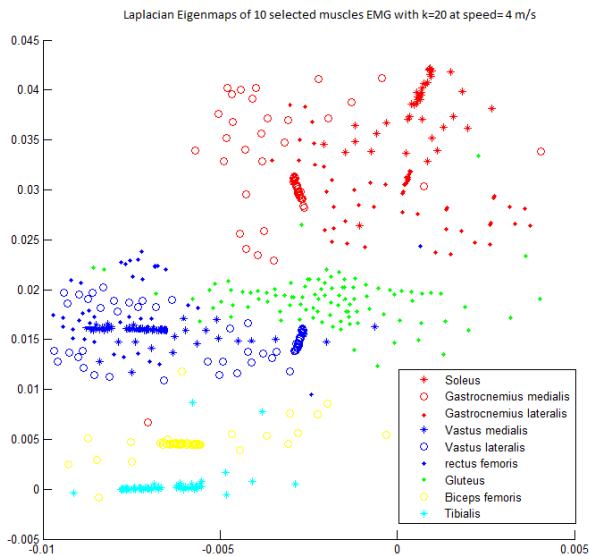


Fig. 5 Laplacian algorithm of 10 selected muscles with $k=20$ at speed 4 m/s

IV. CONCLUSION

This study applied manifold learning and Laplacian Eigenmaps algorithm in order to identify various patterns of EMG signals for different muscles at different running speeds. Laplacian Eigenmaps nonlinear dimensionality reduction algorithm is the most appropriate method to reduce the high dimensionality of EMG signals while preserving aspects in time-frequency domain. This work precisely classified EMG, which affected the dynamics of a human musculoskeletal system at different running speeds. The results of our simulation can be used to investigate the contribution of each muscle to body mass-center accelerations, applicable in the humanoid control, gait analysis, physical therapy, and injury biomechanics. The results of this study can provide important insights into human movement understanding and its application for robotics research.

ACKNOWLEDGMENT

The authors would like to acknowledge Simbios, the National NIH Center for Biomedical Computation at Stanford University, for providing the motion data for this study. They would like to thank California State University Long Beach Office of Research and Sponsored Programs for providing financial support to complete this study.

REFERENCES

- [1] Z. Kourtzi, H. H. Bühlhoff, M. Erb, and W. Grodd, "Object-selective responses in the human motion area MT/MST," *Nature neuroscience*, vol. 5, pp. 17-18, 2002.
- [2] D. B. Chaffin, G. Andersson, and B. J. Martin, *Occupational biomechanics*: Wiley New York, 1999.
- [3] A. Bashashati, M. Fatourechhi, R. K. Ward, and G. E. Birch, "A survey of signal processing algorithms in brain-computer interfaces based on electrical brain signals," *Journal of Neural engineering*, vol. 4, p. R32, 2007.
- [4] O. Khatib, E. Demircan, V. De Sapio, L. Sentis, T. Besier, and S. Delp, "Robotics-based synthesis of human motion," *Journal of Physiology-Paris*, vol. 103, pp. 211-219, 2009.
- [5] N. S. Pollard, J. K. Hodgins, M. J. Riley, and C. G. Atkeson, "Adapting human motion for the control of a humanoid robot," in *Robotics and Automation, 2002. Proceedings. ICRA'02. IEEE International Conference on*, 2002, pp. 1390-1397.
- [6] S. K. Au, P. Bonato, and H. Herr, "An EMG-position controlled system for an active ankle-foot prosthesis: an initial experimental study," in *Rehabilitation robotics, 2005. ICORR 2005. 9th international conference on*, 2005, pp. 375-379.
- [7] S. Kim, J. E. Clark, and M. R. Cutkosky, "iSprawl: Design and tuning for high-speed autonomous open-loop running," *The International Journal of Robotics Research*, vol. 25, pp. 903-912, 2006.
- [8] R. Jimenez-Fabian and O. Verlinden, "Review of control algorithms for robotic ankle systems in lower-limb orthoses, prostheses, and exoskeletons," *Medical engineering & physics*, vol. 34, pp. 397-408, 2012.
- [9] M. A. Oskoei and H. Hu, "Myoelectric control systems—A survey," *Biomedical Signal Processing and Control*, vol. 2, pp. 275-294, 2007.
- [10] M. G. Gazendam and A. L. Hof, "Averaged EMG profiles in jogging and running at different speeds," *Gait & posture*, vol. 25, pp. 604-614, 2007.
- [11] A. Hof, H. Elzinga, W. Grimmus, and J. Halbertsma, "Speed dependence of averaged EMG profiles in walking," *Gait & posture*, vol. 16, pp. 78-86, 2002.
- [12] D. Winter and H. Yack, "EMG profiles during normal human walking: stride-to-stride and inter-subject variability," *Electroencephalography and clinical neurophysiology*, vol. 67, pp. 402-411, 1987.
- [13] R. H. Gabel and R. A. Brand, "The effects of signal conditioning on the statistical analyses of gait EMG," *Electroencephalography and Clinical Neurophysiology/Evoked Potentials Section*, vol. 93, pp. 188-201, 1994.
- [14] V. von Tscharnar, B. Goepfert, and B. M. Nigg, "Changes in EMG signals for the muscle tibialis anterior while running barefoot or with shoes resolved by non-linearly scaled wavelets," *Journal of biomechanics*, vol. 36, pp. 1169-1176, 2003.
- [15] T. F. Novacheck, "The biomechanics of running," *Gait & posture*, vol. 7, pp. 77-95, 1998.
- [16] B. Chen and N. Wan, "Determining EMG embedding and fractal dimensions and its application," in *Engineering in medicine and biology society, 2000. Proceedings of the 22nd annual international conference of the IEEE*, 2000, pp. 1341-1344.
- [17] H. Kyröläinen, P. V. Komi, and A. Belli, "Changes in Muscle Activity Patterns and Kinetics With Increasing Running Speed," *The Journal of Strength & Conditioning Research*, vol. 13, pp. 400-406, 1999.
- [18] J. B. Tenenbaum, V. De Silva, and J. C. Langford, "A global geometric framework for nonlinear dimensionality reduction," *science*, vol. 290, pp. 2319-2323, 2000.
- [19] M. Belkin and P. Niyogi, "Laplacian Eigenmaps and Spectral Techniques for Embedding and Clustering," in *NIPS*, 2001, pp. 585-591.
- [20] S. R. Hamner and S. L. Delp, "Muscle contributions to fore-aft and vertical body mass center accelerations over a range of running speeds," *Journal of biomechanics*, vol. 46, pp. 780-787, 2013.
- [21] G. Lu, J.-S. Brittain, P. Holland, J. Yianni, A. L. Green, J. F. Stein, et al., "Removing ECG noise from surface EMG signals using adaptive filtering," *Neuroscience letters*, vol. 462, pp. 14-19, 2009.
- [22] C. Marque, C. Bisch, R. Dantas, S. Elayoubi, V. Brosse, and C. Perot, "Adaptive filtering for ECG rejection from surface EMG recordings," *Journal of electromyography and kinesiology*, vol. 15, pp. 310-315, 2005.
- [23] E. Lashgari, M. Jahed, and B. Khalaj, "Manifold learning for ECG arrhythmia recognition," in *Biomedical Engineering (ICBME), 2013 20th Iranian Conference on*, 2013, pp. 126-131.
- [24] K. Englehart, B. Hudgins, P. A. Parker, and M. Stevenson, "Classification of the myoelectric signal using time-frequency based representations," *Medical engineering & physics*, vol. 21, pp. 431-438, 1999.
- [25] A. Phinyomark, P. Phukpattaranont, and C. Limsakul, "Feature reduction and selection for EMG signal classification," *Expert Systems with Applications*, vol. 39, pp. 7420-7431, 2012.

- [26] D. De Ridder and R. P. Duin, "Locally linear embedding for classification," *Pattern Recognition Group, Dept. of Imaging Science & Technology, Delft University of Technology, Delft, The Netherlands, Tech. Rep. PH-2002-01*, pp. 1-12, 2002.
- [27] T. M. Cover and P. E. Hart, "Nearest neighbor pattern classification," *Information Theory, IEEE Transactions on*, vol. 13, pp. 21-27, 1967.
- [28] B. Scholkopf and K.-R. Mullert, "Fisher discriminant analysis with kernels," *Neural networks for signal processing IX*, vol. 1, p. 1, 1999.
- [29] G. H. John and P. Langley, "Estimating continuous distributions in Bayesian classifiers," in *Proceedings of the Eleventh conference on Uncertainty in artificial intelligence*, 1995, pp. 338-345.
- [30] P. Langley and S. Sage, "Induction of selective Bayesian classifiers," in *Proceedings of the Tenth international conference on Uncertainty in artificial intelligence*, 1994, pp. 399-406.
- [31] R. Kohavi, "A study of cross-validation and bootstrap for accuracy estimation and model selection," in *Ijcai*, 1995, pp. 1137-1145.
- [32] Scholkmann, F., Boss, J. and Wolf, M., 2012. An efficient algorithm for automatic peak detection in noisy periodic and quasi-periodic signals. *Algorithms*, 5(4), pp.588-603.